

Combining hazard, exposure and vulnerability data to predict historical United States hurricane losses

Alexander F. Vessey^{1*}, Alexander J. Baker^{2,3*}, Vernie Marcellin-Honore², and James Michelin²

¹AXA XL, 20 Gracechurch Street, London, United Kingdom

²Department of Meteorology, University of Reading, Reading, United Kingdom

³National Centre for Atmospheric Science, Reading, United Kingdom

Correspondence to: Alexander F. Vessey (alecvessey@hotmail.co.uk) and Alexander J. Baker (alexander.baker@reading.ac.uk)

Abstract. Hurricanes are among the most destructive natural hazards globally. The widely used Saffir–Simpson scale is an effective public-communication tool, but it is based on a single hazard quantity (wind speed) and has low skill in representing historical economic losses. Accurate risk assessment requires hazard, exposure, and vulnerability information. We present a statistical model to predict losses from North Atlantic hurricanes making landfall in the United States using optimally weighted, normalised-rank quantities describing hazard, exposure, and vulnerability. The model significantly outperforms single-parameter predictions, including landfall wind-speed maxima and central-pressure minima. Root-mean-square error between observed losses and losses predicted from landfall wind speed alone is U.S.\$ 35.6 bn, which our model reduces to U.S.\$ 7.0 bn. To improve the characterisation of risk, we introduce a loss-based ‘Hurricane Predictive Loss Scale’ to more directly link hurricane characteristics and landfall to financial impacts. These results demonstrate that integrating exposure and vulnerability data with hazard observations yields skilful estimates of historical hurricane losses, and our approach may help assess how loss from a forecast landfall may rank among historical events. This work is applicable to other cyclone-prone regions and highlights the critical need for open-source exposure and vulnerability data to advance climate risk understanding.

Significance statement. Hurricanes are a destructive natural hazard. Historically, however, their Saffir–Simpson categories and losses are not well correlated. We combined hazard, exposure, and vulnerability data to predict losses from landfalling hurricanes for the United States. Our model significantly reduces errors between predicted and observed losses and is more skilful than hazard-only predictions. Additionally, we developed a novel loss-based hurricane classification scheme to aid risk management.

32 1 Introduction

33 Intense tropical cyclones are the most impactful meteorological hazard worldwide ((Aon, 2025; World Meteorological
34 Organization, 2021). Between 1980 and 2024, global economic losses due to tropical cyclone landfalls totals U.S.\$ 2.9 tn
35 (National Oceanographic and Atmospheric Administration, 2024), through extreme wind, storm surge and rainfall. Generally,
36 extreme wind induces building damage (Ibrahim et al., 2024) and storm surge and intense rainfall cause fatalities (Rappaport,
37 2014). Improving our understanding of hurricane risk is essential to mitigating impacts through long-term policies, such as
38 strengthened building codes, and short-term preparedness measures, such as early-warning systems.

39 Skilful hurricane damage assessments are challenging and uncertain, as the impacted area may be large and building damage
40 highly site-specific. Nonetheless, damage assessment reports over the last century agree that the most financially impactful
41 U.S. hurricanes include the Great Miami Hurricane (1926), Katrina (2005), and Harvey (2017) (Delforge et al., 2025; Grinsted
42 et al., 2019; Muller et al., 2025; National Centers for Environmental Information, 2025; Weinkle et al., 2018). There is also
43 evidence that hurricane-related economic losses have increased over time (Grinsted et al., 2019; Klotzbach et al., 2022b),
44 highlighting the urgency of understanding impacts and losses to enhance disaster preparedness and support mitigation.
45 However, uncertainties in studies of high-impact landfalling events are high compared with basin-wide metrics of cyclone
46 activity (Emanuel, 2011). Additionally, significant uncertainty remains over how hurricane-related impacts will evolve in a
47 warming climate (Knutson et al., 2020; Meiler et al., 2025), including U.S. landfalls (Jewson, 2023), so understanding the key
48 factors responsible for, and which therefore help predict, losses regionally is critical.

49 Recent work has demonstrated skilful multi-year predictions of North Atlantic hurricane activity and U.S. hurricane damage,
50 but individual high-damage events, particularly those occurring during periods of generally low activity, are not well predicted
51 (Lockwood et al., 2023). Each hurricane-related loss is the result of a unique combination of meteorological and socioeconomic
52 factors, and quantifying hurricane risk requires an understanding of hazard, exposure and vulnerability (Ward et al., 2020).
53 Hazard quantities describe a hurricane’s physical characteristics, including intensity, duration, size, and associated perils such
54 as storm surge and rainfall-induced flooding. Exposure variables capture the location and value of affected assets, including
55 residential, commercial, and industrial buildings within the storm’s footprint. Vulnerability metrics reflect assets’ susceptibility
56 to damage, influenced by construction materials, design and age. To account for these factors, open-source catastrophe models,
57 such as CLIMADA (Aznar-Siguan and Bresch, 2019), HAZUS (Federal Emergency Management Agency, 2024a) and OASIS
58 LMF (Oasis Loss Modelling Framework, 2025), simulate a hurricane’s track and estimate damage based on exposure and
59 vulnerability at the landfall location. However, case-study evidence suggests such models significantly underestimate historical
60 loss estimates for hurricanes (König, 2017) and other storm types, such as European windstorms (Welker et al., 2021). For
61 hurricanes, this lack of skill may be due to the representation of hazard footprints (e.g., wind, precipitation and storm surge),

62 resulting from the insufficient resolution of forecast model data or reliance on a parametric wind field (e.g., Holland et al.,
63 2010). More complex, proprietary catastrophe models are typically used by (re-)insurers.

64 North Atlantic hurricanes are categorised using the Saffir–Simpson Hurricane Wind Scale, which indicates damage potential
65 based on 1-minute near-surface wind speed (Kelman, 2013). This scale is a key tool for public communication of hurricane
66 risk (Cass et al., 2023). However, as it is based on a single hazard quantity, it does not predict damage sufficiently skilfully
67 (Bloemendaal et al., 2021). At landfall, central sea-level pressure minima are more strongly correlated with normalised
68 historical hurricane damage than wind-speed maxima (Klotzbach et al., 2020; Klotzbach et al., 2022a), likely due to central
69 pressure being physically related to both hurricane maximum wind speed and size (Chavas et al., 2025). To characterise
70 potential hurricane damage, there are calls to modify the Saffir–Simpson scale (Wehner and Kossin, 2024) and develop multi-
71 hazard and multidisciplinary (i.e., hazard, exposure and vulnerability) equivalents (Tripathy et al., 2024), to understand
72 hurricane impacts and how risk may evolve in a warming climate (Camelo and Mayo, 2021; Gori et al., 2025; Tripathy et al.,
73 2024; Ward et al., 2020).

74 To develop a hurricane classification more closely aligned with observed damage, Bloemendaal et al. (2021) devised a
75 ‘Tropical Cyclone Severity Scale’, which categorises hurricanes by incorporating wind speed, storm surge and accumulated
76 rainfall. Hurricanes ranked by this scale corresponded better with historical losses compared with the Saffir–Simpson scale,
77 but several events were still mis-represented and assigned a low category despite causing significant damage. For example,
78 Hurricane Sandy (2012) resulted in an estimated U.S.\$ 70 bn in normalised economic losses, but its classification was only
79 changed from category 1 in the Saffir–Simpson scale to category 2 in the ‘Tropical Cyclone Severity Scale’ (Bloemendaal et
80 al., 2021). Other studies have attempted to develop skilful multidisciplinary scales (i.e., not only hazard information).
81 Pilkington and Mahmoud (2016) used an artificial neural network model to forecast the economic impact from hurricanes
82 using hazard and exposure data, including landfall location, population affected, wind speed, central pressure, precipitation
83 and storm surge. Baldwin et al. (2023) showed the importance of differences in vulnerability between conurbations and rural
84 areas for accurately modelling hurricane risk across the Philippines, stressing the importance of including a vulnerability layer
85 to link a given wind speed to a percentage of exposed assets destroyed. These studies highlight the importance of accounting
86 for multiple risk factors.

87 Focussing on historical U.S. landfalling hurricanes, this study examines numerous hurricane hazard, exposure and vulnerability
88 quantities to determine whether the inclusion of socioeconomic data into a statistical loss-prediction model improves our ability
89 to predict losses. Additionally, we developed a novel, loss-based hurricane classification scheme, which, if applied prior to
90 forecast landfall, may communicate potential losses more accurately than Saffir–Simpson, thereby providing a usable
91 preparedness tool for governments, disaster management agencies, and the financial sector. Here, ‘usable’ means skilfully

92 communicating where the expected loss would rank in the context of historical events and revising this estimation as hurricane
93 forecasts evolve (i.e., with shorter lead times). This information could support effective preparedness by response agencies
94 and adequate capital mobilisation by financial institutions and stakeholders. We address the following research questions:

95

96 ● Which single hazard, exposure and vulnerability variable(s) exhibit the highest correlation(s) to historical U.S.
97 hurricane losses?

98 ● How skilful is a combination of hazard, exposure and vulnerability data in predicting historical U.S. losses compared
99 with hazard-only predictions?

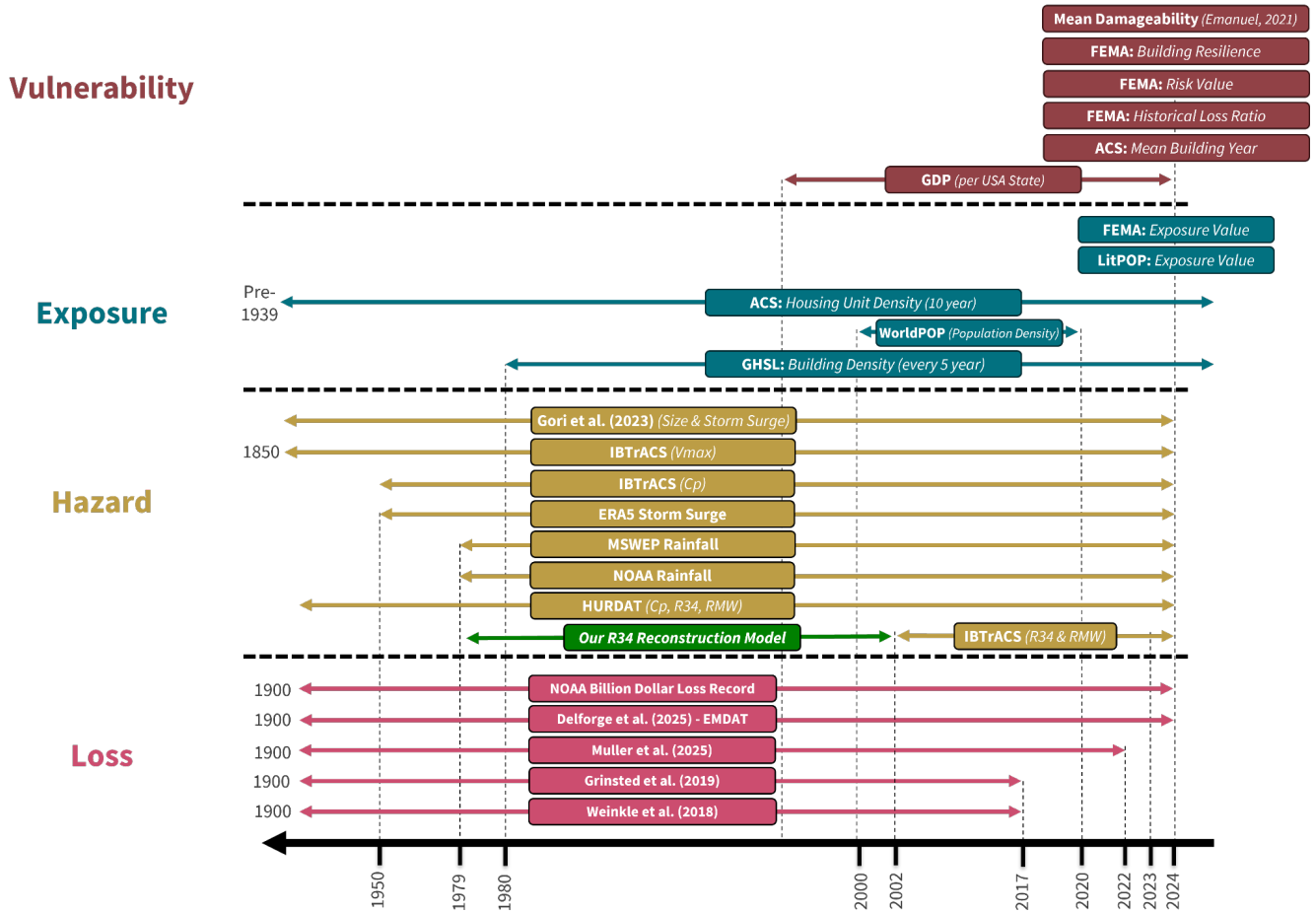
100 ● How skilfully does a loss-based hurricane classification scale represent historical U.S. losses?

101

102 This paper is structured as follows: datasets and methods are described in section 2, results presented in sections 3–5, with a
103 novel loss-based hurricane scale evaluated in section 6, and discussion and conclusions presented in section 7.

105 2.1 Data

106 In this section, we describe the datasets used to provide loss, hazard, exposure and vulnerability information for historical
 107 hurricanes affecting the U.S. Fig. 1 provides a summary of these datasets and the temporal coverage spanned by each.



108

109 *Figure 1. Schematic overview of datasets used in this study. Hazard, exposure and vulnerability predictors were combined,*
 110 *with loss estimates being the predictand. Time-invariant exposure and vulnerability datasets are shown with no arrows. Note*
 111 *that the x-axis timeline is not linear. Table S1 provides additional information and references for these datasets.*

112 2.1.1. Normalised historical hurricane losses

113 Various sources of historical hurricane loss information exist, but no consensus reference dataset. We collated the following
 114 published sources: Grinsted et al. (2019), Muller et al. (2025), National Centers for Environmental Information (2025),
 115 Weinkle et al. (2018), and the Emergency Events Database (EM-DAT; Delforge et al., 2025). These datasets differ in temporal
 116 coverage, reporting methodology, treatment of damage components, and inclusion of historical hurricane events (Fig. 1; Table
 117 1). To maximise sample size, we combined these datasets and, for events with multiple loss estimates, these were averaged to
 118 avoid treating any dataset preferentially and help capture uncertainty. For hurricanes which made multiple landfalls, losses
 119 were averaged from the two sources—Grinsted et al. (2019) and Muller et al. (2025)—that provide per-landfall losses.
 120 Collating data in this way yielded 134 loss estimates for landfalling (including multiple landfalls) hurricanes for the period
 121 1979–2024, of which all variables are available for 106 events (Table 1).

122 *Table 1. Summary of hurricane loss datasets, the number of U.S. hurricane landfalls (including multiple landfalls) during*
 123 *1979–2024 for which a loss estimate is available, and the subset of these landfalls for which all predictors (hazard, exposure*
 124 *and vulnerability) are available.*

| Dataset reference | Dataset coverage | Landfalling hurricanes (1979–2024) with a loss estimate | Landfalling hurricanes (1979–2024) with all hazard, exposure, vulnerability and loss data |
|---|-------------------------|--|--|
| National Centers for Environmental Information (2025) (\geq bn loss) | 1850–present | 58 | 21 |
| EM-DAT (Delforge <i>et al.</i> , 2025) | 1900–present | 74 | 57 |

| | | | |
|-------------------------------|-----------|-----|-----|
| Muller <i>et al.</i> (2025) | 1979–2022 | 33 | 33 |
| Weinkle <i>et al.</i> (2018) | 1900–2018 | 59 | 57 |
| Grinsted <i>et al.</i> (2019) | 1900–2018 | 102 | 76 |
| All data sources | 1979–2024 | 134 | 106 |

125 Economic loss estimates must be calibrated to present-day levels of damage, including adjustment factors to account for
126 temporal changes in inflation, wealth and building density (Weinkle et al., 2018). Typically, normalisation is based on country-
127 level adjustments and assumes building density may be represented by residential housing changes. Regional variations in
128 these factors, temporal changes in building vulnerability or commercial building density, and the impacts of climate change
129 may not be accounted for (Muller et al., 2025). Each dataset we used (Table 1) provides un-normalised and normalised
130 hurricane loss estimates. However, uncertainty arises due to the differing normalisation methodologies and reference years
131 between datasets. To ensure consistency, we used un-normalised data and applied a unified normalisation approach, based on
132 Weinkle et al. (2018) and Muller et al. (2025), where loss estimates were adjusted using country-level inflation and real-
133 wealth-per-housing-unit factors (both as of 2024), and a county-level housing unit density factor (Eq. 1).

$$134 \quad L_{2024} = L_y \cdot \frac{I_{2024}}{y} \cdot \frac{W}{Hn_{1+\frac{(2024-y)}{y}}} \cdot Hn_{1+\frac{(2024-y)}{y}} \quad (\text{Eq. 1})$$

135 where L is loss per hurricane (and year), y , I is inflation, W is real national wealth per housing unit, and Hn is housing unit
136 density. I was determined using the annual implicit price deflator for gross domestic product (GDP) for the period 1979–2024
137 (U.S. Bureau of Economic Analysis, 2023). Hn density was determined within R34 using U.S. housing unit data (U.S. Census

138 Bureau, 2024). W was quantified using an estimate of current-cost net stock of fixed assets and consumer durable goods (U.S.
139 Bureau of Economic Analysis, 2025).

140 2.1.2. Hazards

141 Hurricane track location, intensity and size information was obtained from the International Best Track Archive for Climate
142 Stewardship (IBTrACS) v04r01 (Gahtan et al., 2024), provided by the National Hurricane Center. For each historical
143 hurricane, we obtained 1-minute sustained maximum wind speed, v_{\max} , minimum central sea-level pressure, c_p , translation
144 speed, radius of maximum wind (from the storm centre), RMW, and the outermost radii of 34-, 50- and 64-knot wind speeds
145 from the storm centre), respectively, R34, R50 and R64. Each quantity was determined at the timestep before the storm centre
146 crosses over land, so atmospheric fields are minimally impacted by land-surface interactions. However, IBTrACS data are
147 incomplete (i.e., not all hazard variables are available at every timestep for every hurricane). Therefore, we supplemented
148 IBTrACS with data from NOAA’s HURDAT2 reanalysis (Landsea and Franklin, 2013)—specifically, the ‘U.S. Hurricane
149 Impacts / Landfalls’ table of landfall information collected by NOAA reconnaissance aircraft (Hurricane Research Division,
150 2025) and from Gori et al. (2023). Where data are missing in IBTrACS, HURDAT2 data were substituted, if available. Where
151 data are available in IBTrACS and HURDAT2 at a given timestep, HURDAT2 data were prioritised.

152 Storm surge and rainfall cause damage through coastal and inland flooding. In this study, historical hurricane storm tide
153 (maximum storm surge and tidal height) data were taken from the storm surge residual product (Copernicus Climate Change
154 Service, 2022), derived using the Global Tide and Surge Model version 3.0 (Kernkamp et al., 2011; Wang et al., 2021) forced
155 by European Centre for Medium-Range Weather Forecasts’ fifth-generation reanalysis (ERA5; Hersbach et al., 2020). This
156 provides hourly reconstructed historical storm tide height from 1950–present. Storm tide residual is calculated as the difference
157 between the total water level and simulated storm-tide elevation, including the influence of storm surge and tide. Storm tide
158 may be larger in the hours before or after a hurricane makes landfall, depending on antecedent tidal height. To account for this,
159 we defined the maximum storm tide residual as the maximum along the U.S. coastline within a 1,000 km radius of the
160 hurricane’s central coordinate and 24 hours before and after a hurricane makes landfall. An example maximum storm tide
161 residual for Hurricane Katrina (2005) is shown in Fig. S1.

162 Historical hurricane-related rainfall footprints were derived from the Multi-Source Weighted-Ensemble Precipitation
163 (MSWEP) dataset (Beck et al., 2019), which assimilates gauge observations and satellite data to reconstruct 3-hourly rainfall
164 1979–present. For each hurricane, we determined total accumulated rainfall, maximum 3-hourly rain rate, and maximum total
165 rain accumulation per grid-point along the track, each within a 500-km radius of the hurricane centre (location taken from

166 IBTrACS) at each timestep. An example rainfall accumulation footprint for Hurricane Katrina is shown in Fig. S2. This chosen
167 radius is based on previous research (e.g., Stansfield and Reed, 2023), although a fixed radius may lead to some overestimation
168 of cyclone-related precipitation (Stansfield et al., 2020). To complement MSWEP, the maximum rainfall accumulation along
169 each hurricane track was collated from National Oceanographic and Atmospheric Administration (2025), providing single
170 maximum rainfall accumulation values, although not allowing differentiation between multiple landfalls with this dataset.

171 This study considers only landfalling hurricanes, excluding bypassing hurricanes. It is difficult to obtain a comparable measure
172 of hurricane intensity for a bypassing event because its intensity, measured close to the system centre, is over ocean and may
173 therefore be relatively high compared with a directly landfalling event. It is necessary to avoid introducing such an artifact into
174 our statistical model.

175 *2.1.3. Exposure*

176 We took county-level building value information across the U.S. from the National Risk Index (Federal Emergency
177 Management Agency, 2024b), derived from Hazus 6.1 (Federal Emergency Management Agency, 2024a), providing 2022-
178 relative valuations per county based on the 2020 U.S. Census. Building values are time-invariant. Near present-day (2019)
179 building value was quantified using the LitPOP dataset (Eberenz et al., 2020), providing global aggregated building value
180 estimates at a 1-km spatial resolution. Building value estimates vary between the two datasets; hence, we used two building
181 value datasets.

182 We also used decadal, county-level housing unit density data (U.S. Census Bureau, 2024), available 1950–present, as well as
183 semi-decadal building density estimates from the Global Human Settlement Layer (GHSL), providing built-up surface area
184 data derived from Sentinel-2 composite and Landsat satellite imagery from 1975–present at 1-km spatial resolution (Pesaresi
185 and Politis, 2023). Annual gridded population density data between 2000 and 2020 at 1-km spatial resolution were obtained
186 from WorldPop (2018). For hurricane landfalls outside the temporal coverage of GHSL and WorldPop, we used data for the
187 closest available year. Therefore, a limitation to highlight is that we overestimate population density for pre-2000 events.

188 *2.1.4. Vulnerability*

189 Structural vulnerability—the susceptibility of buildings to damage—is influenced by building age, often used as a proxy for
190 building condition and resilience, and related to changes in building codes (regulated construction standards that include a
191 minimal resistance to extreme weather). We used county-level average building age data (U.S. Census Bureau, 2024) and a

192 county-level indicator of building resistance to extreme weather (Federal Emergency Management Agency, 2025). We also
193 used county-level Hurricane Risk Score and Hurricane Historical Loss Ratio data from Federal Emergency Management
194 Agency (2024b) and Zuzak et al. (2021). Hurricane Risk Score is defined as the average social vulnerability (i.e., extent to
195 which specific social groups are disproportionately susceptible to hurricane impacts) and community resilience (i.e., capacity
196 to prepare for, withstand, and recover from hurricane hazards), and is given as a percentage. Hurricane Historical Loss Ratio
197 is defined as the percentage of a location’s exposed value damaged by past hurricanes. We quantified the mean Hurricane Risk
198 Score and Hurricane Historical Loss Ratio across all counties within several hurricane radii (R34, R50 and R64—see section
199 2.2.). GDP data for each affected U.S. state per year, indicating a state’s resilience resources, for the period 1998–2024 (U.S.
200 Bureau of Economic Analysis, 2025) were used, and 1998 GDP values were applied to pre-1998 events.

201 Hurricane wind vulnerability may also be expressed as a logistic–cubic wind–damage function, relating wind speed to the
202 fractional value of assets lost. This study uses a simple quantification of this (Eq. 2 and Eq. 3), which was deduced by Emanuel
203 (2011).

$$204 \quad f = \frac{v_n^3}{1+v_n^3}, \quad (\text{Eq. 2})$$

205 where f is the fraction of the property value lost and v_n is defined as:

$$206 \quad v_n = \frac{[(v-v_{\text{thresh}}),0]}{v_{\text{half}}-v_{\text{thresh}}}, \quad (\text{Eq. 3})$$

207 where v is maximum wind speed, and v_{thresh} and v_{half} are the thresholds at which no asset damage and half asset damage occur,
208 respectively. Building characteristics (e.g., construction type and age) influence vulnerability curves, and Vickery et al. (2006)
209 and Federal Emergency Management Agency (2024a) suggest v_{half} values in the range 120–160 kts. In this study, damage
210 estimates were computed for historical hurricanes using this single vulnerability function for all buildings, with $v_{\text{thresh}} = 40$ kts
211 and $v_{\text{half}} = 140$ kts. However, weaker systems may be damaging, such as tropical depression Allison (2001), modelling suggests
212 v_{half} may be as low as ~50 kts (Federal Emergency Management Agency, 2024a). Multiple vulnerability functions for different
213 building types cannot be applied due to incomplete localised building characteristic data. Instead, asset damage potential was
214 applied to 1-dimensional LitPOP exposure and GHSL building density data within each hurricane footprint to estimate the

215 exposure value and number of buildings damaged. At each timestep, v_{\max} was used with Eq. 2 and Eq. 3 (Emanuel, 2011) and
216 the extracted exposure and building density, allowing v_{\max} to vary with time.

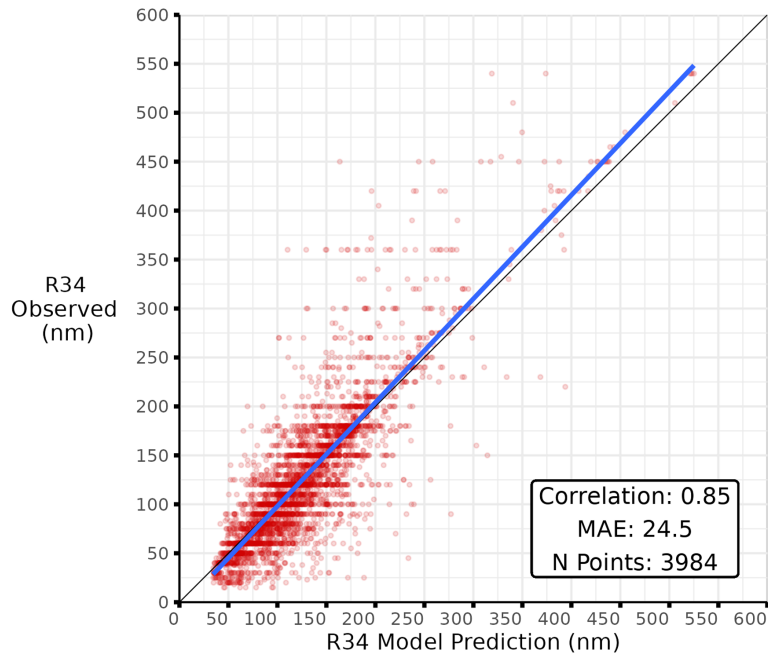
217 2.2. Methods

218 2.2.1. Statistical estimation of hurricane size

219 Hurricane size (i.e., R34, R50 and R64) data are only available in IBTrACS from 2002 onwards. This is a significant constraint
220 for studies of impact, as size information is needed to determine the region impacted by an event—i.e., its footprint. The
221 exposure and vulnerability impact footprints derived in this study require hurricane size estimates. To estimate size prior to
222 2002 and extend the sample of landfalling hurricanes for this study, we developed a skilful random-forest statistical model to
223 estimate R34, R50 and R64 for each hurricane and at each timestep, based on v_{\max} , RMW, c_p and latitude (Fig. 2), with RMW
224 found to be the most influential predictor. When R34 estimates from this model are compared with R34 observations from
225 2002 onwards, a Spearman’s correlation coefficient, ρ , of 0.85 and a mean absolute error (MAE) of 24.5 nm were found (Fig.
226 2). This evaluation used a leave-one-out approach (i.e., the prediction model was trained on all observations except one, and
227 skill evaluated on the left-out observation) across 3,984 timesteps (for which R34, v_{\max} , RMW, c_p and latitude within IBTrACS
228 are not missing). There is a slight underestimation of R34 at lower values and slight overestimation at higher values, but the
229 model overall performs well. This statistical modelling is a skilful supplement to missing IBTrACS data (Fig. 2 and Fig. S3)
230 and allows storm size estimation back to 1979, which more than doubles our historical hurricane event sample size. Prediction
231 models were also developed to estimate R50 and R64 for historical storms, where observations are available, with evaluation
232 shown in Fig. S3.

233 From 1979 to 2002, however, there are instances where RMW data are missing from IBTrACS (v_{\max} , RMW, c_p and latitude
234 are less often missing). So, for these timesteps, we either substituted the missing RMW value from the corresponding value
235 from HURDAT2 or obtained the RMW value from reconstructions of Gori et al. (2023). Reconstructed RMW from Gori et al.
236 (2023) is based on the hurricane wind model of Chavas et al. (2025) and ERA5 data. Of all 3-hourly timesteps where a hurricane
237 is over land between 1979 and 2002 (approximately 10,000 timesteps), approximately 25% timesteps have a missing RMW
238 estimate from each of these three datasets. In these instances, we replaced the missing value with the RMW from the previous
239 timestep. Although this introduces uncertainty, R34, R50 and R64 estimates from the random-forest model using RMW

240 estimates from previous timesteps are also a function of c_p , v_{max} and latitude, quantities that are much less frequently missing
241 in IBTrACS, and these constrain our R34 statistical model even when using substituted RMW values.



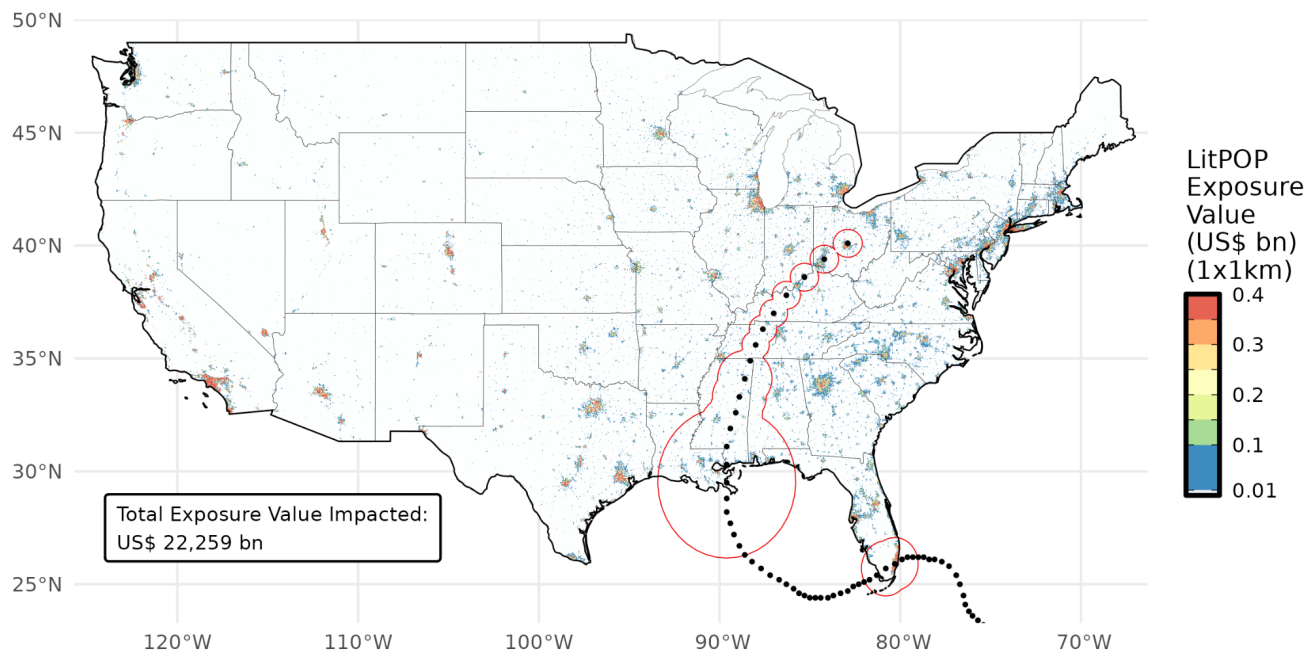
242

243 *Figure 2. Comparison of estimated and observed hurricane R34 (unit is nautical miles, nm) for the period 2002–2023. Our*
244 *random-forest statistical model uses hurricane v_{max} , RMW, c_p and latitude as R34 predictors.*

245 *2.2.2. Extracting hurricane-centred exposure and vulnerability footprints*

246 For each hurricane, exposure and vulnerability data were extracted within the R34, R50 and R64 radii at each timestep, and
247 accumulated to create two impact footprints: i) along the full hurricane track where $v_{max} > 34$ kts (Fig. 3) and ii) from the

248 immediate landfall location (i.e., up to 12 hours after landfall). Hurricanes weaken over land, so obtaining two impact footprints
249 captures the immediate landfall, where intensity influences impacts most strongly, and the full hurricane track.



250

251 *Figure 3. Example LitPOP exposure value impact footprint of Hurricane Katrina (2005). Hurricane locations from IBTrACS*
252 *every three hours are shown as black dots, with the R34 radius around the hurricane centre indicated by the red lines. Harvey*
253 *made landfall in southern Florida, traversed the Gulf of Mexico, and made a second landfall in Louisiana.*

254 2.2.3. Predictive statistical approaches

255 We assessed the skill of three independent statistical approaches to predict hurricane loss, each based on the same set of inputs.
256 These are: (i) a weighted combined-rank framework, (ii) a linear-regression framework, and (iii) a random-forest decision-tree
257 framework. Our target predictand is average loss per hurricane, derived from multiple datasets (see section 2.1.1.). Overall,
258 106 hurricanes, for which all risk variables could be quantified (Table 1), were used to train our predictive model. To evaluate
259 the skill of the linear regression and random-forest predictive models, leave-one-out cross-validation was used, where each
260 input case was treated once as the test case and the model trained on the remaining cases. The leave-one-out approach is better
261 suited to evaluating the skill of single predictions than, for example, k-fold cross-validation, where input data are split into

262 training subsets. For the weighted combined-rank framework, which determines the combined loss rank from various hazard,
263 exposure and vulnerability ranks, such validation is inappropriate, as the combined-rank approach does not require training
264 data. Instead, optimal combinations of weights between -10 and 10 were determined for each combination of input variables,
265 to minimise a cost function, which in this case was the model root-mean-square error (RMSE) between predicted and observed
266 hurricane loss rank.

267 Two approaches were considered for representing input variables: raw values and ranked values. As input variables span
268 disparate ranges (e.g., c_p spans 900–1000 hPa; LitPOP exposure spans U.S.\$ 10 M to 1 tn), raw values were normalised to the
269 same scale as ranked values $1-n$ (i.e., 1–106). In this normalisation, each variable was linearly rescaled to assign the maximum
270 value a score of 1 and minimum a score of 106, with intermediate values mapped proportionally between these bounds. Linear
271 and normalised input predictor ranks were derived, with rank 1 corresponding to the costliest event and rank 106 to the least
272 costly. To predict each hurricane’s loss, the equivalent predicted loss rank and observed loss rank were identified, with the
273 loss from that observed hurricane being attributed to that predicted loss rank.

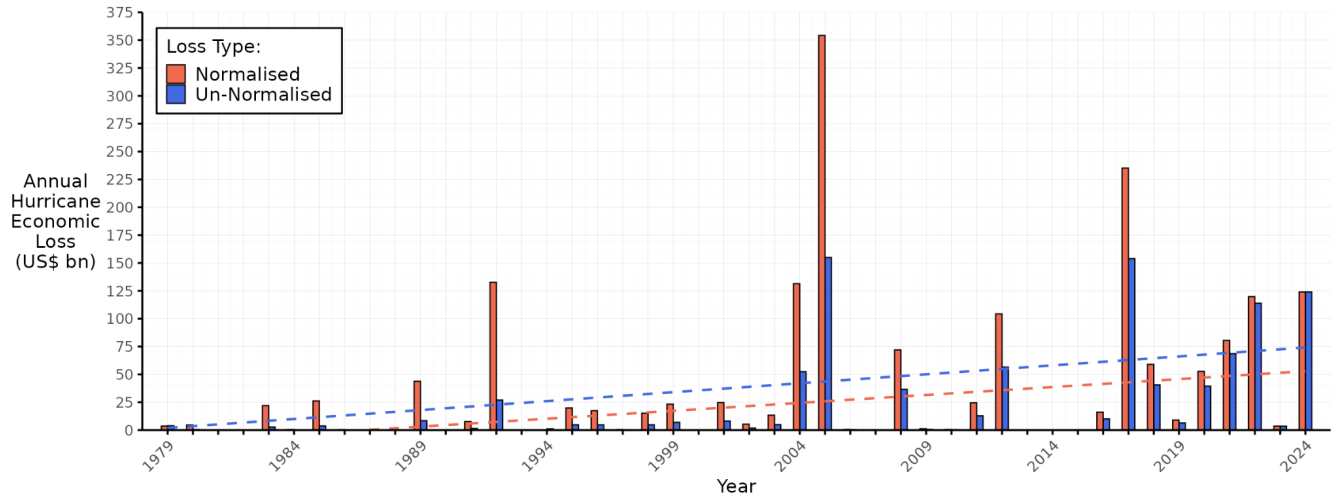
274 We quantified model performance with the Spearman correlation coefficient, ρ , testing the ordering of prediction according to
275 correlation between ranked values (i.e., whether one event is more damaging than another), Pearson correlation coefficients,
276 r , testing non-ranked correlation, and RMSE. Spearman’s ρ and RMSE were used as ρ is a good indicator of the capability of
277 accurately predicting loss rank, but not suitable for identifying cases where large differences occur in the loss prediction of a
278 single hurricane.

279 **3 Historical relationship between hurricane wind speed and loss**

280 Hurricane-related losses across the U.S. have generally increased over time and exhibit large interannual variability (Fig. 4).
281 The most destructive year for losses was 2005, with U.S.\$ 153 bn in un-normalised (and approximately U.S.\$ 350 bn in
282 normalised) loss. The most damaging event was Hurricane Katrina (Fig. 5), although uncertainty is evident across available
283 loss datasets (Table 1). If Katrina occurred today, loss may be in the range of U.S.\$ 190–290 bn (Fig. 5). Katrina, however, is
284 one of numerous high-impact hurricanes whose v_{\max} -based Saffir–Simpson category at landfall is at odds with the magnitude
285 of associated loss (Bloemendaal et al., 2021). Katrina was a category-3 landfall, despite causing unprecedented, record-
286 breaking damage (Fig. 5). Other cases whose damage is mismatched with their Saffir–Simpson category include category-1
287 Hurricane Sandy (2012) and category-2 Hurricane Ike (2008), which each caused substantial losses (Fig. 5). Additionally,
288 Hurricane Harvey (2017) was a category-4 landfall and the second-most damaging hurricane, but its loss is uncertain, with

289 estimates between U.S.\$ 90–190 bn. The historical record reveals the limitation of an event’s Saffir–Simpson category in
290 conveying its loss.

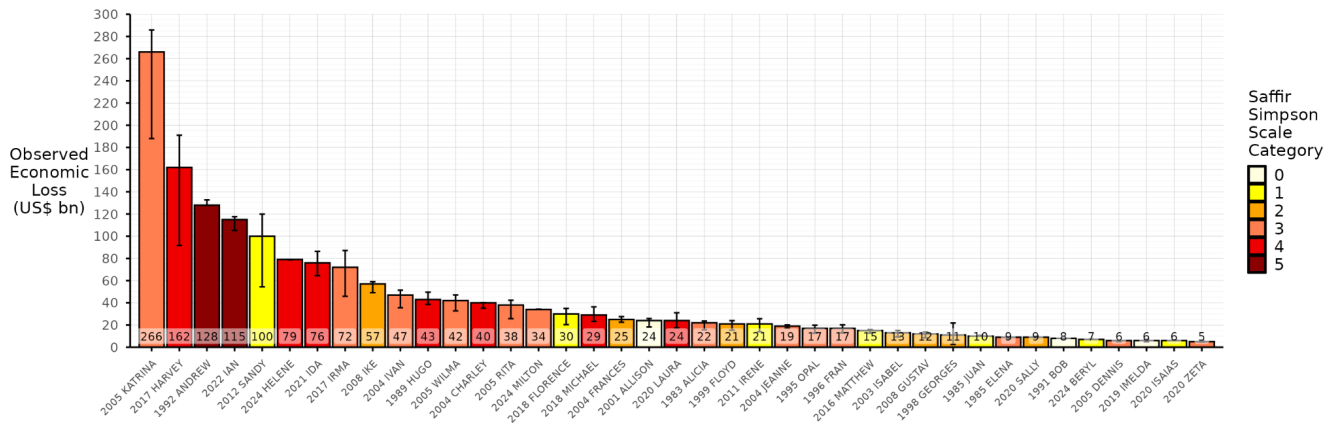
291



292

293 *Figure 4. Average historical U.S. hurricane-related losses, (red) normalised to 2024 and (blue) un-normalised by inflation,*
294 *wealth and housing unit density (blue). Dashed lines indicate upward linear trends.*

295

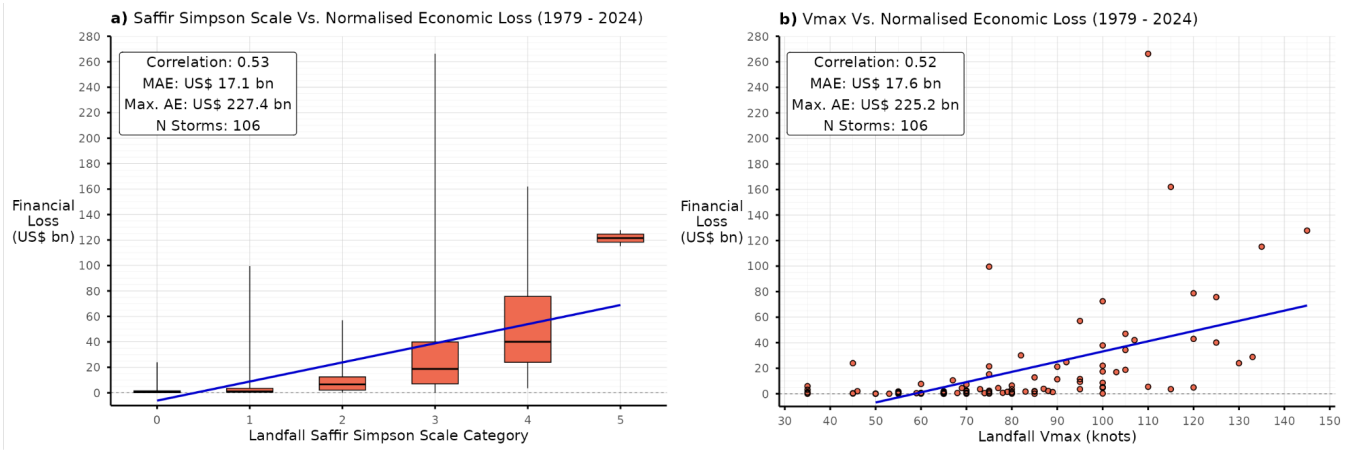


296

297 *Figure 5. Average loss per hurricane, normalised to 2024, for loss events exceeding U.S.\$ 5 bn. Error bars indicate the range*
 298 *in loss estimates across datasets (Fig. 1 and Table 1) and colour indicates landfall Saffir–Simpson category.*

299 Although loss generally increases with the Saffir–Simpson landfall category and therefore wind speed (Fig. 5), the Saffir–
 300 Simpson scale has limited skill in predicting loss (Fig. 6a), with a correlation of $\rho = 0.53$ across 106 events (RMSE = U.S.\$
 301 17.1 bn when using Saffir–Simpson category to predict loss rank and associated loss using a linear model). Using v_{\max} to
 302 predict normalised hurricane loss yields a correlation of $\rho = 0.52$ (RMSE = U.S.\$ 17.6 bn), which is slightly lower (Fig. 6b)
 303 and consistent with Klotzbach et al. (2020). Notably, landfall v_{\max} is significantly less skilful at predicting loss for more extreme
 304 storms, with generally higher error at more extreme v_{\max} values (Fig. 6b), which is particularly problematic as an inaccurate
 305 forecast for these more intense storms would produce larger errors in loss. The relationship between v_{\max} and loss is potentially
 306 nonlinear but spread, and therefore error, in loss generally increases with v_{\max} . Performing a rank correlation between observed

307 loss and loss predicted from v_{\max} reveals significant spread (and heteroscedasticity) across the observed range (Fig. 7a), and
308 this is found for all events as well as those where exceeds U.S.\$ 1 bn (Fig. S4).



310 *Figure 6. Average economic hurricane financial loss (normalised to 2024) versus a) Saffir–Simpson category and b) landfall*
311 *v_{\max} of U.S. landfalls over the period 1979–2023. Blue lines indicate linear fits and an indication of goodness of fit is given in*
312 *each legend: mean absolute error (MAE), absolute error (AE), and sample size, N .*

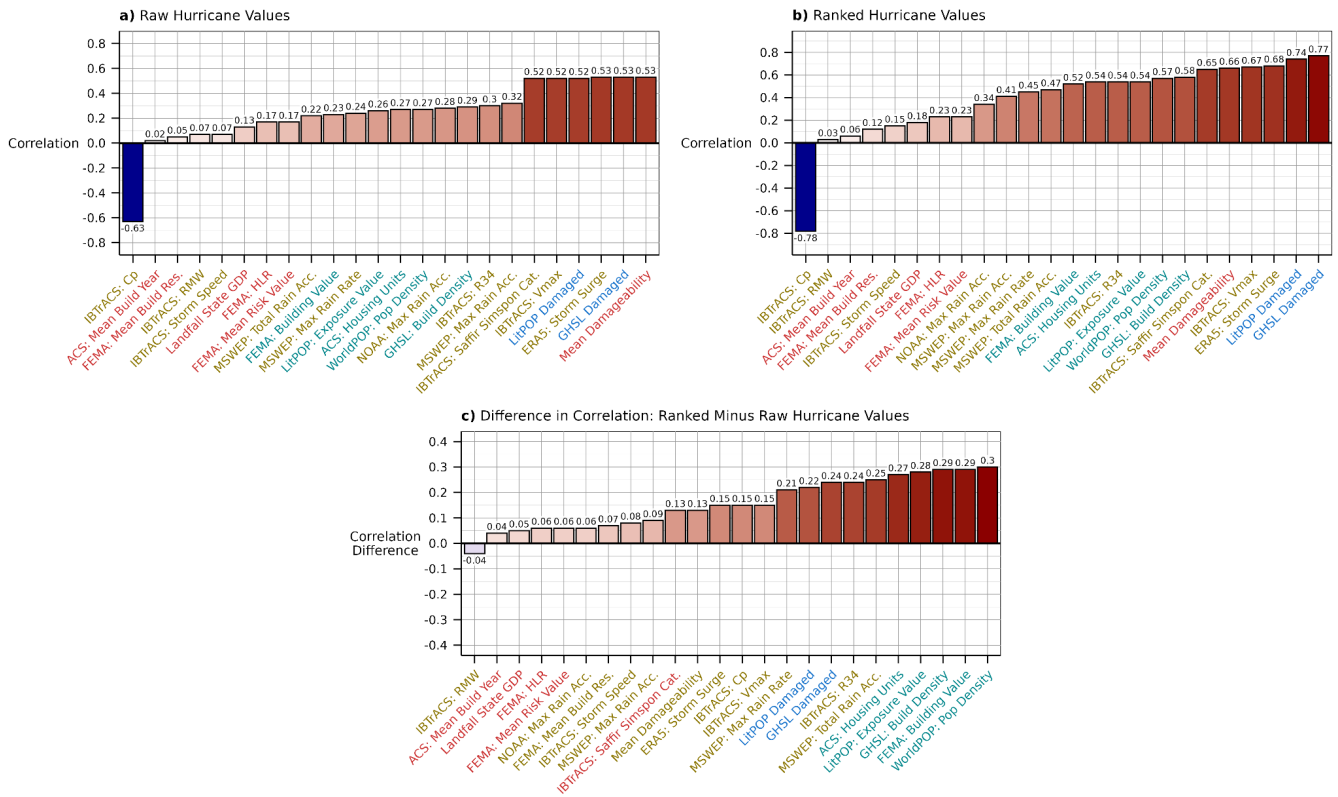
313 4 Historical relationships between multiple hazard, exposure and vulnerability variables and loss

314 We next analysed linear correlations between single predictors and historical hurricane loss over the period 1979–2024, using
315 both raw (Fig. 7a) and rank (Fig. 7b) values. This analysis demonstrates that high prediction skill may be obtained across
316 numerous hazard, exposure and vulnerability hurricane quantities, with landfall c_p rank yielding the highest correlation ($r = -$
317 0.78), followed by GHSL building density damage percentage ($r = 0.77$) and LitPOP exposure value damage percentage ($r =$
318 0.74) (Fig. 7a). Overall, using the value rank per storm yields higher correlations than using raw values (Fig. 7c), particularly
319 for exposure predictors, because using ranks normalises to a linear scale, suggesting that landfall attribute ranks may provide
320 more skilful loss predictions. This complements the analysis of Klotzbach et al. (2022b), who showed that landfall c_p better
321 correlates with loss rank than v_{\max} or accumulated cyclone energy. Here, we further show that landfall c_p outperforms other

322 hazard variables and that landfall exposure and vulnerability variables yield higher correlations with loss rank than landfall
323 v_{max} .

324 In this study, several hazard variables at landfall (v_{max} , c_p , storm tide, R34, translation speed, and RMW) remain unchanged,
325 but variables quantified within a hurricane footprint depend on chosen hurricane size metric (i.e., R34, R50 or R64), and those
326 quantified along-track depend on timeframe (i.e., full track or 12 hours post landfall). For landfall variables with significant
327 correlations to loss (i.e., ≥ 0.3), a 12-hour post-landfall track yields similar (or somewhat higher) correlation compared with
328 using the full track where winds exceed 34 kts (Fig. S5a). This indicates that including the full track, where winds weaken
329 over land, reduces correlation. (Studies of inland impacts using full-track analysis may need to cope with lower skill than
330 landfall-focussed studies.) A notable exception is the percentage of damaged GHSL building density, which has a strong
331 correlation using the full track ($\rho = 0.78$ using R34 and $\rho = 0.79$ using R50). Correlations are generally higher when considering
332 normalised rather than un-normalised loss (Fig. S5b). Additionally, rank correlations are similar when using R34 and R50 to

333 define impact radius, but correlations using R64 are lower (Fig. S5c). R64 is typically less than 100 nm, which may be too
 334 small to capture hurricane impacts, especially for lower-resolution data (e.g., county-level housing unit data).



335

336 *Figure 7. Pearson's correlation coefficients between historical hurricane landfall predictors, quantified at landfall and within*
 337 *12 hours of landfall, and averaged loss for the period 1979–2024. Shown are (a) raw values versus loss, (b) predictor rank*
 338 *values versus loss, and (c) the coefficient difference between using raw versus ranked values (i.e., ranked minus raw*
 339 *correlations). Note that the x-axes differ between the panels due to correlation ordering. Colours indicate whether the variable*
 340 *is a hazard (yellow), exposure (blue) or vulnerability (red) variable (refer to Fig. 1). Note that c_p is inversely related to*
 341 *hurricane intensity and therefore negatively correlated with damage.*

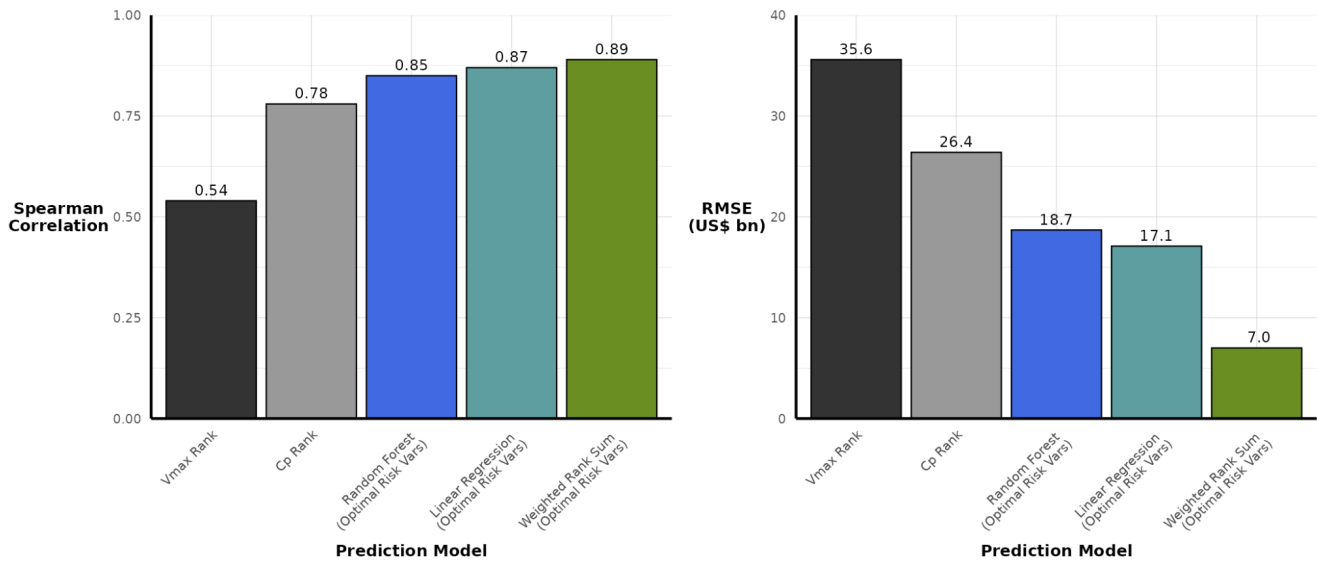
342 **5 Statistical prediction of historical hurricane loss**

343 Using landfall v_{max} rank to predict storm loss, by assigning the loss from the equivalent loss rank, yields $\rho = 0.54$ and RMSE
 344 = U.S.\$ 35.6 bn (Fig. 8), so v_{max} has limited skill predicting historical loss. Hurricanes Katrina (2005) and Harvey (2017),

345 which were category-3 and category-4 landfalls, respectively (Fig. 4), are among the most underestimated losses despite being
346 the two most damaging events since 1979 (Fig. 9a). Furthermore, using v_{\max} alone leads to loss predictions exceeding U.S.\$
347 30 bn for several less-damaging (\leq U.S.\$ 10 bn) events (Fig. 9a), including Michael (2018), Laura (2020), Dennis (2005),
348 Andrew (1992; second landfall) and Idalia (2023). Our analysis (Fig. 7) and recent work (Klotzbach et al., 2020; Klotzbach et
349 al., 2022a) show landfall c_p to be the most skilful single hazard predictor for historical loss, and using landfall c_p rank to predict
350 loss rank improves this correlation ($\rho = 0.78$ and RMSE = U.S.\$ 26.4 bn) (Fig. 8). However, several events, across a range of
351 observed losses, remain poorly predicted: Andrew (1992), Michael (2018), Rita (2005), Hugo (1989), Dennis (2005), Allen
352 (1980) and Idalia (2023) are all overestimated (Fig. 9b). This greater predictive skill of c_p over v_{\max} is likely due to the physical
353 pressure–wind balance intrinsic to hurricanes (Chavas et al., 2017), but intensity metrics alone cannot accurately model loss.

354 We now combine landfall hazard, exposure and vulnerability quantities to derive more skilful models to predict historical
355 hurricane loss, using three statistical approaches: multiple linear regression, random-forest, and weighted combined rank (Fig.
356 8). Using a random-forest model based on the optimal combination of hazard, exposure and vulnerability predictors is
357 significantly skilful ($\rho = 0.85$; RMSE = U.S.\$ 18.7 bn), with a slight improvement obtained from using a linear-regression
358 model ($\rho = 0.87$; RMSE = U.S.\$ 17.1 bn) (Fig. 8). Further skill is obtained when using a weighted combined-sum approach (ρ
359 = 0.89; RMSE = U.S.\$ 7.0 bn), representing a large decrease in RMSE when compared to using c_p and v_{\max} (Fig. 8). Overall,

360 effectively combining hazard, exposure and vulnerability predictors is found to significantly reduce RMSE by 67% compared
361 with using landfall v_{\max} rank alone, and by 55% when using landfall c_p rank alone (Fig. 8).



362

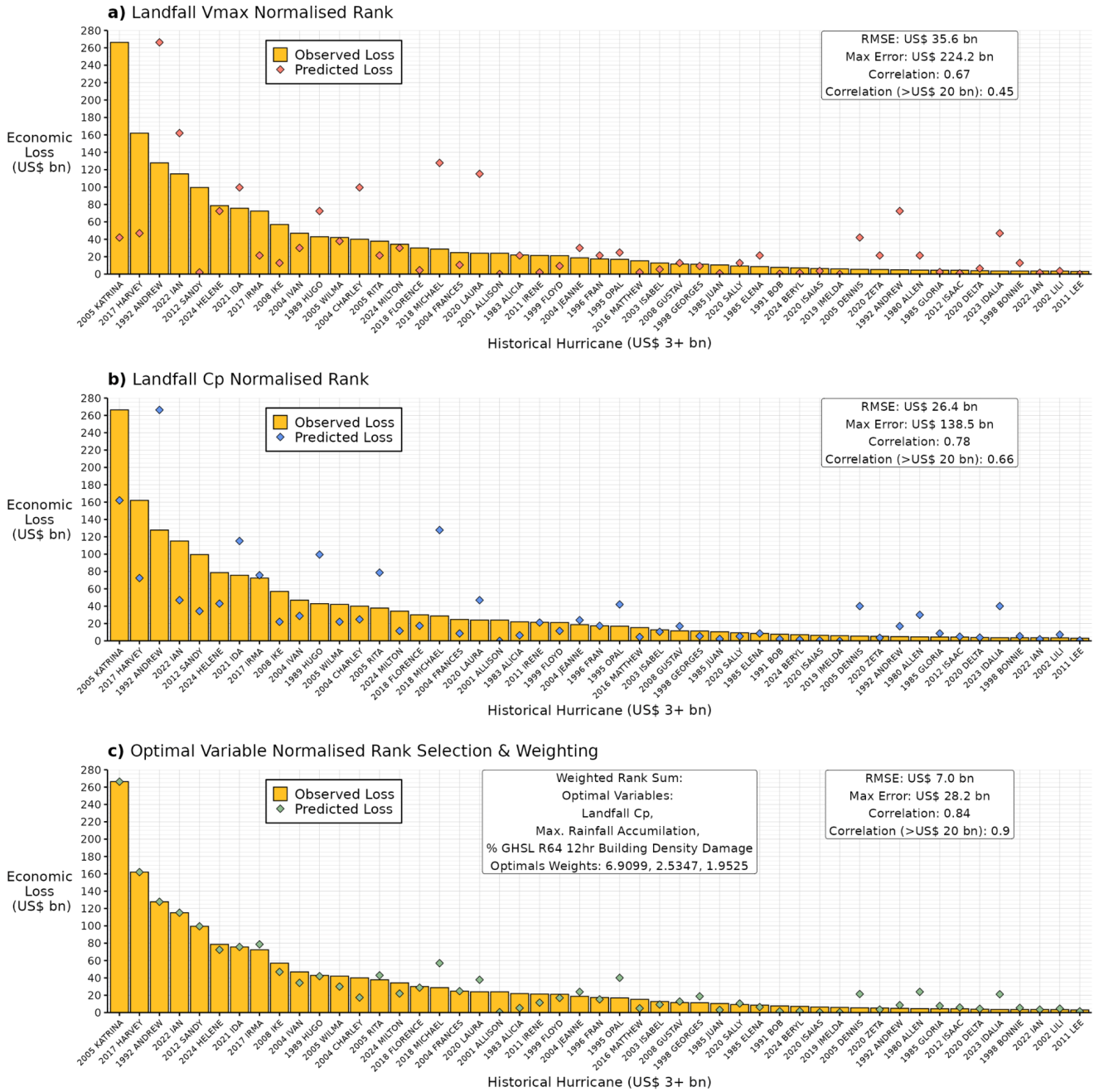
363 *Figure 8. The a) Spearman's correlation coefficient, ρ , and b) root mean squared error (RMSE) of each tested historical*
364 *hurricane loss-prediction model.*

365 This optimal model uses the combined normalised ranks of landfall c_p , maximum rainfall accumulation, and the percentage of
366 total GHSL building density loss within R64 of the hurricane centre and within 12 hours of landfall (Fig 8; Fig. 9c). This model
367 includes two hazard quantities representing hurricane wind and inland flooding intensity (c_p and rainfall), with hurricane radius
368 implicitly included in the percentage of total GHSL building density damage (with storms with larger R64 having higher
369 impacted building density values). This also includes exposure values of impacted building density and applies a vulnerability
370 function, by determining the percentage of damaged buildings proportional to v_{\max} (at each timestep). The inclusion of building
371 density within R64 indicates some prediction skill from capturing the inner region of a hurricane, where wind-induced damage
372 to buildings may be highest, but only in combination with other factors. Overall, this model demonstrates the extent to which
373 loss prediction skill can be improved when accounting for hazard, exposure and vulnerability.

374 Across our sample of 106 historical hurricanes, this prediction model has the lowest RMSE (U.S.\$ 7.0 bn) when hazard,
375 exposure and vulnerability predictors are ranked and summed, while also applying optimal weights (Fig. 8c). Moreover, for

376 highly damaging historical hurricanes (\geq U.S.\$ 20 bn), $\rho = 0.9$, which is significantly higher than using only landfall v_{\max} ($\rho =$
377 0.45) or c_p ($\rho = 0.66$) (Fig. 9). Our optimal model results in the five most-damaging hurricanes (Katrina, Harvey, Andrew, Ian,
378 and Sandy) being ordered according to observed losses and thus well captured, and higher-loss events (\geq U.S.\$ 20–80 bn)
379 overall are skilfully predicted. However, some discrepancies remain. The largest errors include hurricanes Michael (2018),
380 Opal (1995) and Allen (1980), all of which have a high landfall c_p rank (i.e., high intensity) but relatively low loss. Overall,

381 this model is markedly more skilful than using intensity metrics (landfall v_{max} and c_p) to predict historical losses (Fig. 8 and
 382 Fig. 9).



383

384 *Figure 9. Comparisons of landfall predictor rank with loss rank to predict past hurricane loss given past loss observations,*
 385 *using (a) landfall v_{max} rank, (b) landfall c_p rank, and (c) optimally selected and weighted (refer to Fig. 7) hazard, exposure*
 386 *and vulnerability linear rank variables at landfall. Yellow bars indicate observed historical hurricane loss, and the coloured*
 387 *diamonds indicate predicted historical hurricane loss. Note that the optimal risk predictors and their optimal weights are*
 388 *given in panel (c).*

389 **6 A loss-based hurricane classification**

390 The Saffir–Simpson scale is an effective communication tool and a key component of early-warning dissemination (Camelo
 391 and Mayo, 2021; Oliver-Smith, 2020; Wehner and Kossin, 2024), but, being based on v_{max} alone, does not correspond
 392 adequately with historical loss ranking (Fig. 4, Fig. 5). Based on our analyses, we devised a loss-based hurricane categorisation,
 393 termed the ‘Hurricane Predictive Loss Scale’ (HPLS). We intend this scale to complement the Saffir–Simpson scale, as well
 394 as published work (Bloemendaal et al., 2021; Pilkington and Mahmoud, 2016), and be a classification scheme that may be
 395 used by stakeholders, particularly (re-)insurance, to predict loss.

396 Since 1900, 39% of landfalling hurricanes have been category 1, with 12% and 3% being category 4 and 5, respectively (Table
 397 S2). We applied the observed relative proportions in each Saffir–Simpson category to averaged historical loss data since 1979
 398 (Table 1) to derive historical loss categories (Table 2) for the HPLS. As examples, a hurricane with loss less than U.S.\$ 1.3 bn
 399 is a ‘loss category 1’ event and an event causing loss greater than U.S.\$ 119.5 bn is a ‘loss category 5’ event.

400 *Table 2. Percentage of landfalling historical storms within each Saffir–Simpson category since 1900 (Hurricane Research*
 401 *Division, 2025). Loss category thresholds used to define the proposed HPLS.*

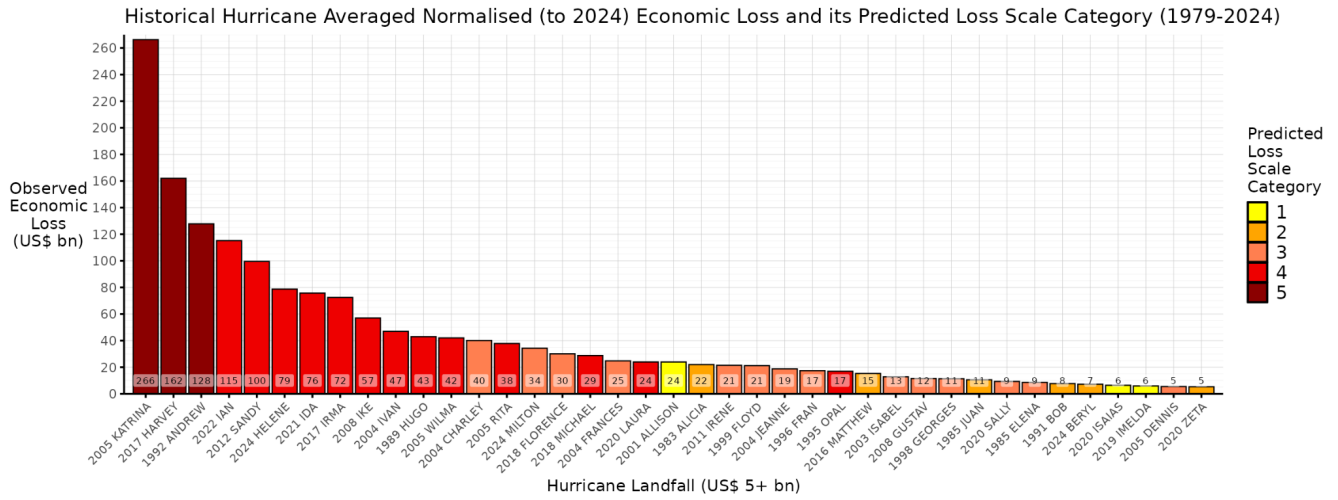
| Saffir–Simpson category | Frequency | % of all hurricanes | v_{max} threshold (kts) | HPLS loss category threshold (U.S.\$ bn) |
|--------------------------------|------------------|----------------------------|---|---|
| 1 | 84 | 38.9 | 64-83 | 0-1.3 |

| | | | | |
|---|----|------|---------|------------|
| 2 | 54 | 25.0 | 83-96 | 1.3-5.3 |
| 3 | 46 | 21.3 | 96-113 | 5.3-29.5 |
| 4 | 26 | 12.0 | 113-136 | 29.5-119.5 |
| 5 | 6 | 2.8 | 136+ | 119.5+ |

402 Using our skilful hurricane loss-prediction model, we determined the HPLS loss category derived from the predicted losses
403 for each historical hurricane (Fig. 9c and Fig. 10). The ranks of the most damaging hurricanes (Katrina, Harvey, and Andrew)
404 are correctly predicted as being ‘loss category 5’, and the next most damaging storms (Ian to Wilma) are ‘loss category 4’
405 events, with losses between U.S.\$ 115-42 bn (Fig. 10). Hurricane Sandy (2012), which is under-categorised by the Saffir–
406 Simpson scale (category 1) and the ‘Tropical Cyclone Severity Scale’ (Bloemendaal et al., 2021) (category 2), is a ‘loss
407 category 4’ event in our scheme. Combining hazard, exposure and vulnerability quantities and loss-based categorisation is
408 more skilful for many cases than is possible based only on hazard information.

409 The most damaging hurricane that is misrepresented by the HPLS scheme is Hurricane Charley (2004), whose observed loss
410 (U.S.\$ 40.1 bn) is underpredicted by our model (Fig. 10). Charley should be ‘loss category 4’ (Fig. 4 and Table 2), but its
411 predicted loss (~U.S.\$ 20 bn) falls in ‘loss category 3’. Additionally, tropical storm Allison (2001) is assigned to ‘loss category
412 1’, which stands out as a poor model prediction (Fig. 10). Overall, we found 74 events (70%) are correctly classified by the
413 HPLS (Table 3). However, 28 events (26%) are misrepresented by ± 1 ‘loss category’ and 4 (4%) are misrepresented by ± 2

414 'loss categories' (Table 3). By comparison, Saffir–Simpson categories represent just over half (55%) of events correctly, and
 415 31%, 12% and 2% are misrepresented by ± 1 , ± 2 and ± 3 'loss categories', respectively (Table 3).



416

417 *Figure 10. Predicted 'loss category' of each historical landfalling hurricane, using the optimal prediction model (Fig. 9c) and*
 418 *the HPLS (Table 2).*

419

420 *Table 3. Quantified differences between Saffir–Simpson category or predicted ‘loss category’ using our model (Fig. 9c) and*
 421 *the observed ‘loss category’ from the HPLS (i.e., derived from observed loss).*

| Difference from observed ‘loss category’ | Saffir–Simpson category | Predicted ‘loss category’ |
|---|--------------------------------|----------------------------------|
| 0 (i.e., correct prediction) | 58 (55%) | 74 (70%) |
| ±1 | 33 (31%) | 28 (26%) |
| ±2 | 15 (12%) | 4 (4%) |
| ±3 | 5 (2%) | 0 (0%) |

422

423 **7 Summary and discussion**

424 This study explored statistical relationships between historical U.S. hurricane-related losses and quantities describing hazard,
 425 exposure and vulnerability, and makes two contributions. First, we determined whether the inclusion of socioeconomic
 426 information into a predictive model for loss from U.S. landfalls yields significant additional skill compared with using only
 427 hazard information. For historical hurricanes, we derived storm-centred hazard, exposure and vulnerability quantities, and
 428 limited our analysis to cases for which observed loss estimates are available and hurricane radius is either observed or could
 429 be skilfully estimated statistically from other observed size information. Second, we devised a loss-based hurricane
 430 classification scheme to allow rapid, skilful assessment of the loss potential of forecast events, which is intended for use by

431 stakeholders in hurricane risk, including governmental agencies and the (re-)insurance sector, and complements existing
432 classification schemes.

433 7.1 Key results and limitations

434 7.1.1 *Integrated hazard, exposure, and vulnerability data predict historical hurricane losses more skilfully than hazard* 435 *data alone*

436 Although historical losses generally increase with landfall wind speed (and Saffir–Simpson category), hazard information
437 alone has insufficient skill in predicting historical losses, with a large RMSE across all events, a finding which substantiates
438 previous research (Klotzbach et al., 2020; Klotzbach et al., 2022a). We find various hurricane-centred hazard, exposure and
439 vulnerability quantities correlate significantly with losses (i.e., $r > 0.5$), but using a weighted-rank-sum approach to optimally
440 combine these predictors yields markedly more skilful loss predictions ($\rho = 0.89$ for all storms). This high correlation between
441 loss observations and predictions, with a significantly reduced RMSE of U.S.\$ 7.0 bn, improves the predicted loss rank of the
442 most impactful historical cases. This optimal prediction model was derived by determining the weighted sum of normalised
443 ranks of landfall c_p , maximum rainfall accumulation, and the percentage of total GHSL building density damage within R64
444 and within 12 hours of landfall. This model includes two hazard attributes representing hurricane intensity (c_p and rainfall),
445 building density impacted, and applies a vulnerability function (percentage of building damage proportional to v_{\max}). For this
446 model, important limitations are related to the observational uncertainties within the input predictor data, as well as in the
447 target variable. There is significant variance among loss estimates for historical events. Additional uncertainty stems from the
448 lack of complete cyclone size information prior to 2002, which is not completely mitigated by our statistical estimation
449 approach and could impact skill for pre-2002 landfalls. A key data gap is the availability of vulnerability information and its
450 temporal granularity. Lastly, historical loss uncertainty necessitated consideration of multiple datasets and averaging losses
451 where required.

452 Studies based on physical climate model outputs provide evidence of significant interannual to decadal variability in damage
453 (Lavender et al., 2022) and substantial inter-model uncertainty (Meiler et al., 2023). Projected increases in vulnerable assets,
454 assuming no adaptation, may worsen damage to a greater extent than physical hazard changes (Gettelman et al., 2018).
455 Regional vulnerability, particularly building characteristics, is important, and regional factors are accounted for in high-
456 resolution catastrophe models (e.g., Eberenz et al., 2021) and synthetic tropical cyclone models (e.g., Meiler et al., 2022),
457 although results exhibit sensitivity to model setup (Meiler et al., 2025). Open-source catastrophe models may underestimate
458 historical losses (König, 2017; Welker et al., 2021), so a comprehensive intercomparison of such models across historical

459 hurricanes is warranted. While our statistical model may not predict hurricane losses events outside our sample (i.e., loss
460 significantly exceeding that of Hurricane Katrina), it ranks losses in historical context and complements other catastrophe
461 modelling approaches.

462 7.1.2 *A loss-based hurricane scale effectively communicates economic impacts*

463 We devised a ‘Hurricane Predictive Loss Scale’ in which hurricanes are assigned a ‘loss category’. This characterises
464 hurricanes according to economic losses, complementing the Saffir–Simpson scale and prior work (Bloemendaal et al., 2021;
465 Pilkington and Mahmoud, 2016). Our model-predicted ‘loss categories’ matched observed categories (determined from loss
466 data) in 70% of cases, comparing favourably with the Saffir–Simpson scale. An illustrative example is Hurricane Sandy (2012),
467 a lower-intensity, larger-size storm that is assigned ‘loss category 4’, a more appropriate characterisation of the actual loss.
468 The HPLS offers a simple method to embed information about potential losses for forecast landfalls to support decision-
469 making. In (re-)insurance, pooling risk across a diversified portfolio reduces capital costs and increases loss predictability
470 (Ciullo et al., 2023). For hurricanes, however, recent basin-wide (Klotzbach et al., 2022b) and near-coast (Qi et al., 2025;
471 Wang and Toumi, 2021; Zhong et al., 2026) trends in hazards will increasingly challenge risk stakeholders. We therefore
472 anticipate that our scheme will be a useful risk-management tool.

473 **7.2. Outlook**

474 Our study highlights clear data needs. First, vulnerability data of higher spatial and temporal granularity are needed. Using
475 open-source datasets here necessitated a combination of time-varying and time-invariant predictors, which is an area for
476 improvement. The development of such datasets using emerging technologies offers potential—for example, combining
477 machine learning and satellite imagery to describe building attributes and structural vulnerability, and their changes, with
478 higher fidelity. Vulnerability may be economic or social and characterised by economic or demographic data, respectively
479 (Wilson et al., 2022). Second, there is a need for hurricane size information for historical events. This key physical quantity
480 directly determines impacted areas (Wang and Toumi, 2016), and future work to reconstruct wind radii would be considerably
481 beneficial. It is somewhat unclear how climate change may impact the horizontal structure of a hurricane’s wind field.
482 Expansion rates increase with sea-surface warming (Wang et al., 2025), yet outer size is not projected to change over this

483 century (Schenkel et al., 2023). Studies of high-resolution climate models, which adequately capture intensification and
484 horizontal structure (Baker et al., 2024), may help substantiate projections and evaluate their risk implications.

485 There is potential to refine our approach for application to a variety of sectors and stakeholders (Beven et al., 2018). We
486 developed a loss-based classification, but different schemes could be developed for specific sectors. For example,
487 governments, disaster-relief organisations and public-health services may employ classification based on expected fatalities,
488 requiring an understanding of human factors, such as risk perception (Wong-Parodi and Garfin, 2022) and the ability of
489 communities to respond to warnings (Black et al., 2013). Predictions of human impacts could be made following our statistical
490 framework, given adequate historical mortality-burden data for model training. Additionally, our methodology may be applied
491 to other cyclone-prone regions, where necessary data are available. Finally, our predictive model may help quantify hurricane
492 risk changes in a warming climate by its application to simulated future hurricanes, which may be more intense and induce
493 heavier precipitation (Knutson et al., 2020), to quantify how losses may respond to hazard changes and the expected losses
494 due to unprecedented landfalls in regions of significant exposure or vulnerability.

495

496 **8 Acknowledgements**

497

498 AJB is supported by the National Centre for Atmospheric Science and by the nextGEMS (European Union Horizon2020 grant
499 agreement 101003470) and Huracán (NERC–NSF grant agreement NE/W009587/1) projects. Data analysis in this study was
500 facilitated by JASMIN (jasmin.ac.uk), which is operated by the Science and Technology Facilities Council on behalf of the
501 Natural Environment Research Council.

502

503

504 **9 Author contributions**

505

506 AFV and AJB conceived the study. AFV performed data analysis and figure preparation, supported by AJB, VMH and JM.
507 AFV and AJB wrote the manuscript. All authors interpreted results and approved the final draft.

508

509

510 **10 Competing interests**

511

512 The authors declare no competing interests.

513

514

515 **11 Code / data availability**

516

517 IBTrACS data are available from ncei.noaa.gov/products/international-best-track-archive. All other datasets are available from
518 the cited sources. Data analysis and visualisation code is available at github.com/ncas-metoffice-hrcm/hurricane_loss.

519 **References**

520

521 AON: 2025 Climate and Catastrophe Insight, 2025. <https://www.aon.com/en/insights/reports/climate-and-catastrophe-report>.

522 Aznar-Siguan, G. and Bresch, D. N.: CLIMADA v1: a global weather and climate risk assessment platform, *Geosci. Model*
523 *Dev.*, 12, 3085–3097, 10.5194/gmd-12-3085-2019, 2019.

524 Baker, A. J., Vannière, B., and Vidale, P. L.: On the Realism of Tropical Cyclone Intensification in Global Storm-Resolving
525 Climate Models, *Geophysical Research Letters*, 51, e2024GL109841, <https://doi.org/10.1029/2024GL109841>, 2024.

526 Baldwin, J. W., Lee, C.-Y., Walsh, B. J., Camargo, S. J., and Sobel, A. H.: Vulnerability in a Tropical Cyclone Risk Model:
527 Philippines Case Study, *Weather, Climate, and Society*, 15, 503–523, <https://doi.org/10.1175/WCAS-D-22-0049.1>, 2023.

528 Beck, H. E., Wood, E. F., Pan, M., Fisher, C. K., Miralles, D. G., van Dijk, A. I. J. M., McVicar, T. R., and Adler, R. F.:
529 MSWEP V2 Global 3-Hourly 0.1° Precipitation: Methodology and Quantitative Assessment, *Bulletin of the American*
530 *Meteorological Society*, 100, 473–500, <https://doi.org/10.1175/BAMS-D-17-0138.1>, 2019.

531 Beven, K. J., Almeida, S., Aspinall, W. P., Bates, P. D., Blazkova, S., Borgomeo, E., Freer, J., Goda, K., Hall, J. W., Phillips,
532 J. C., Simpson, M., Smith, P. J., Stephenson, D. B., Wagener, T., Watson, M., and Wilkins, K. L.: Epistemic uncertainties and
533 natural hazard risk assessment – Part 1: A review of different natural hazard areas, *Nat. Hazards Earth Syst. Sci.*, 18, 2741–
534 2768, 10.5194/nhess-18-2741-2018, 2018.

535 Black, R., Arnell, N. W., Adger, W. N., Thomas, D., and Geddes, A.: Migration, immobility and displacement outcomes
536 following extreme events, *Environmental Science & Policy*, 27, S32–S43, <https://doi.org/10.1016/j.envsci.2012.09.001>, 2013.

537 Bloemendaal, N., de Moel, H., Mol, J. M., Bosma, P. R. M., Polen, A. N., and Collins, J. M.: Adequately reflecting the severity
538 of tropical cyclones using the new Tropical Cyclone Severity Scale, *Environmental Research Letters*, 16, 014048,
539 10.1088/1748-9326/abd131, 2021.

540 Camelo, J. and Mayo, T.: The lasting impacts of the Saffir-Simpson Hurricane Wind Scale on storm surge risk communication:
541 The need for multidisciplinary research in addressing a multidisciplinary challenge, *Weather and Climate Extremes*, 33,
542 100335, <https://doi.org/10.1016/j.wace.2021.100335>, 2021.

543 Cass, E., Shao, W., Hao, F., Moradkhani, H., and Yeates, E.: Identifying trends in interpretation and responses to hurricane
544 and climate change communication tools, *International Journal of Disaster Risk Reduction*, 93, 103752,
545 <https://doi.org/10.1016/j.ijdr.2023.103752>, 2023.

546 Chavas, D. R., Knaff, J. A., and Klotzbach, P.: A Simple Model for Predicting Tropical Cyclone Minimum Central Pressure
547 from Intensity and Size, *Weather and Forecasting*, 40, 333–346, <https://doi.org/10.1175/WAF-D-24-0031.1>, 2025.

- 548 Chavas, D. R., Reed, K. A., and Knaff, J. A.: Physical understanding of the tropical cyclone wind-pressure relationship, *Nature*
549 *Communications*, 8, 1360, 10.1038/s41467-017-01546-9, 2017.
- 550 Ciullo, A., Strobl, E., Meiler, S., Martius, O., and Bresch, D. N.: Increasing countries' financial resilience through global
551 catastrophe risk pooling, *Nature Communications*, 14, 922, 10.1038/s41467-023-36539-4, 2023.
- 552 Copernicus Climate Change Service: Global sea level change time series from 1950 to 2050 derived from reanalysis and high
553 resolution CMIP6 climate projections, 10.24381/cds.a6d42d60, 2022.
- 554 Delforge, D., Wathelet, V., Below, R., Sofia, C. L., Tonnelier, M., van Loenhout, J. A. F., and Speybroeck, N.: EM-DAT: the
555 Emergency Events Database, *International Journal of Disaster Risk Reduction*, 124, 105509,
556 <https://doi.org/10.1016/j.ijdr.2025.105509>, 2025.
- 557 Eberenz, S., Lüthi, S., and Bresch, D. N.: Regional tropical cyclone impact functions for globally consistent risk assessments,
558 *Nat. Hazards Earth Syst. Sci.*, 21, 393–415, 10.5194/nhess-21-393-2021, 2021.
- 559 Eberenz, S., Stocker, D., Rössli, T., and Bresch, D. N.: Asset exposure data for global physical risk assessment, *Earth System*
560 *Science Data*, 12, 817–833, 10.5194/essd-12-817-2020, 2020.
- 561 Emanuel, K.: Global Warming Effects on U.S. Hurricane Damage, *Weather, Climate, and Society*, 3, 261–268,
562 <https://doi.org/10.1175/WCAS-D-11-00007.1>, 2011.
- 563 Federal Emergency Management Agency: Hazus Hurricane Model Technical Manual, Hazus 6.1, 2024a.
564 https://www.fema.gov/sites/default/files/documents/Hazus_6.1_Hurricane_Model_Technical_Manual.pdf.
- 565 Federal Emergency Management Agency: National Risk Index: Future Risk Technical Documentation, 2024b.
566 https://cepl.law.harvard.edu/wp-content/uploads/2025/03/NRI_Future_Risk_Technical_Document.pdf.
- 567 Federal Emergency Management Agency: Building Code Adoption Tracking, 2025. [https://www.fema.gov/emergency-](https://www.fema.gov/emergency-managers/risk-management/building-science/bcat)
568 [managers/risk-management/building-science/bcat](https://www.fema.gov/emergency-managers/risk-management/building-science/bcat).
- 569 Gahtan, J., Knapp, K., Schreck III, C., Diamond, H., Kossin, J., and Kruk, M. C.: International Best Track Archive for Climate
570 Stewardship (IBTrACS), version 4r01, 2024.
- 571 Gettelman, A., Bresch, D. N., Chen, C. C., Truesdale, J. E., and Bacmeister, J. T.: Projections of future tropical cyclone damage
572 with a high-resolution global climate model, *Climatic Change*, 146, 575–585, 10.1007/s10584-017-1902-7, 2018.
- 573 Gori, A., Lin, N., Schenkel, B., and Chavas, D.: North Atlantic Tropical Cyclone Size and Storm Surge Reconstructions From
574 1950-Present, *Journal of Geophysical Research: Atmospheres*, 128, e2022JD037312, <https://doi.org/10.1029/2022JD037312>,
575 2023.
- 576 Gori, A., Lin, N., Chavas, D., Oppenheimer, M., and Xian, S.: Sensitivity of tropical cyclone risk across the US to changes in
577 storm climatology and socioeconomic growth, *Environmental Research Letters*, 20, 064050, 10.1088/1748-9326/add60d,
578 2025.
- 579 Grinsted, A., Ditlevsen, P., and Christensen, J. H.: Normalized US hurricane damage estimates using area of total destruction,
580 1900–2018, *Proceedings of the National Academy of Sciences*, 116, 23942–23946, 10.1073/pnas.1912277116, 2019.
- 581 Hersbach, H., Bell, B., Berrisford, P., Hirahara, S., Horányi, A., Muñoz-Sabater, J., Nicolas, J., Peubey, C., Radu, R., Schepers,
582 D., Simmons, A., Soci, C., Abdalla, S., Abellan, X., Balsamo, G., Bechtold, P., Biavati, G., Bidlot, J., Bonavita, M., De Chiara,

583 G., Dahlgren, P., Dee, D., Diamantakis, M., Dragani, R., Flemming, J., Forbes, R., Fuentes, M., Geer, A., Haimberger, L.,
584 Healy, S., Hogan, R. J., Hólm, E., Janisková, M., Keeley, S., Laloyaux, P., Lopez, P., Lupu, C., Radnoti, G., de Rosnay, P.,
585 Rozum, I., Vamborg, F., Villaume, S., and Thépaut, J.-N.: The ERA5 global reanalysis, *Quarterly Journal of the Royal*
586 *Meteorological Society*, 146, 1999–2049, <https://doi.org/10.1002/qj.3803>, 2020.

587 Holland, G. J., Belanger, J. I., and Fritz, A.: A Revised Model for Radial Profiles of Hurricane Winds, *Monthly Weather*
588 *Review*, 138, 4393–4401, <https://doi.org/10.1175/2010MWR3317.1>, 2010.

589 Hurricane Research Division: Detailed List of Continental United States Hurricane Impacts/Landfalls, 2025.
590 http://www.aoml.noaa.gov/hrd/hurdat/UShurrs_detailed.html.

591 Ibrahim, H. A., Elawady, A., and Prevatt, D. O.: Empirical hurricane fragility assessment of elevated and slab-on-grade
592 residential houses, *International Journal of Disaster Risk Reduction*, 110, 104663, <https://doi.org/10.1016/j.ijdrr.2024.104663>,
593 2024.

594 Jewson, S.: The Impact of Projected Changes in Hurricane Frequencies on U.S. Hurricane Wind and Surge Damage, *Journal*
595 *of Applied Meteorology and Climatology*, 62, 1827–1843, <https://doi.org/10.1175/JAMC-D-23-0087.1>, 2023.

596 Kelman, I.: Saffir–Simpson Hurricane Intensity Scale, in: *Encyclopedia of Natural Hazards*, edited by: Bobrowsky, P. T.,
597 Springer, Dordrecht, https://doi.org/10.1007/978-1-4020-4399-4_306, 2013.

598 Kernkamp, H. W. J., Van Dam, A., Stelling, G. S., and de Goede, E. D.: Efficient scheme for the shallow water equations on
599 unstructured grids with application to the Continental Shelf, *Ocean Dynamics*, 61, 1175–1188, 10.1007/s10236-011-0423-6,
600 2011.

601 Klotzbach, P. J., Bell, M. M., Bowen, S. G., Gibney, E. J., Knapp, K. R., and Schreck, C. J., III: Surface Pressure a More
602 Skillful Predictor of Normalized Hurricane Damage than Maximum Sustained Wind, *Bulletin of the American Meteorological*
603 *Society*, 101, E830–E846, 10.1175/BAMS-D-19-0062.1, 2020.

604 Klotzbach, P. J., Chavas, D. R., Bell, M. M., Bowen, S. G., Gibney, E. J., and Schreck III, C. J.: Characterizing Continental
605 US Hurricane Risk: Which Intensity Metric Is Best?, *Journal of Geophysical Research: Atmospheres*, 127, e2022JD037030,
606 <https://doi.org/10.1029/2022JD037030>, 2022a.

607 Klotzbach, P. J., Wood, K. M., Schreck III, C. J., Bowen, S. G., Patricola, C. M., and Bell, M. M.: Trends in Global Tropical
608 Cyclone Activity: 1990–2021, *Geophysical Research Letters*, 49, e2021GL095774, <https://doi.org/10.1029/2021GL095774>,
609 2022b.

610 Knutson, T., Camargo, S. J., Chan, J. C. L., Emanuel, K., Ho, C.-H., Kossin, J., Mohapatra, M., Satoh, M., Sugi, M., Walsh,
611 K., and Wu, L.: Tropical Cyclones and Climate Change Assessment: Part II: Projected Response to Anthropogenic Warming,
612 *Bulletin of the American Meteorological Society*, 101, E303–E322, 10.1175/BAMS-D-18-0194.1, 2020.

613 König, N.: Case Study of Hurricane Matthew: Loss Analysis with CLIMADA and Oasis LMF using ECMWF Forecast Data,
614 *Institute of Atmospheric and Climate Sciences, Eidgenössische Technische Hochschule Zürich, Zürich*, 2017.

615 Landsea, C. W. and Franklin, J. L.: Atlantic Hurricane Database Uncertainty and Presentation of a New Database Format,
616 *Monthly Weather Review*, 141, 3576–3592, 10.1175/mwr-d-12-00254.1, 2013.

617 Lavender, S. L., Walsh, K. J. E., Utembe, S., Caron, L.-P., and Guishard, M.: Estimation of maximum seasonal tropical cyclone
618 damage in the Atlantic using climate models, *Natural Hazards*, 110, 1025–1038, 10.1007/s11069-021-04977-2, 2022.

619 Lockwood, J. F., Dunstone, N., Hermanson, L., Saville, G. R., Scaife, A. A., Smith, D., and Thornton, H. E.: A Decadal
620 Climate Service for Insurance: Skillful Multiyear Predictions of North Atlantic Hurricane Activity and U.S. Hurricane
621 Damage, *Journal of Applied Meteorology and Climatology*, 62, 1151–1163, <https://doi.org/10.1175/JAMC-D-22-0147.1>,
622 2023.

623 Meiler, S., Ciullo, A., Kropf, C. M., Emanuel, K., and Bresch, D. N.: Uncertainties and sensitivities in the quantification of
624 future tropical cyclone risk, *Communications Earth & Environment*, 4, 371, 10.1038/s43247-023-00998-w, 2023.

625 Meiler, S., Vogt, T., Bloemendaal, N., Ciullo, A., Lee, C.-Y., Camargo, S. J., Emanuel, K., and Bresch, D. N.: Intercomparison
626 of regional loss estimates from global synthetic tropical cyclone models, *Nature Communications*, 13, 6156, 10.1038/s41467-
627 022-33918-1, 2022.

628 Meiler, S., Kropf, C. M., McCaughey, J. W., Lee, C.-Y., Camargo, S. J., Sobel, A. H., Bloemendaal, N., Emanuel, K., and
629 Bresch, D. N.: Navigating and attributing uncertainty in future tropical cyclone risk estimates, *Science Advances*, 11,
630 eadn4607, 10.1126/sciadv.adn4607, 2025.

631 Muller, J., Mooney, K., Bowen, S. G., Klotzbach, P. J., Martin, T., Philp, T. J., Dhruvkumar, B., Dixon, R. S., and Girmurugan,
632 S. B.: Normalized Hurricane Damage in the United States: 1900–2022, *Bulletin of the American Meteorological Society*, 106,
633 E51–E67, <https://doi.org/10.1175/BAMS-D-23-0280.1>, 2025.

634 National Centers for Environmental Information: U.S. Billion-Dollar Weather and Climate Disasters, 10.25921/stkw-7w73,
635 2025. <https://www.ncei.noaa.gov/access/billions/>.

636 National Oceanographic and Atmospheric Administration: Hurricane Costs, 2024. [https://coast.noaa.gov/states/fast-
637 facts/hurricane-costs.html](https://coast.noaa.gov/states/fast-facts/hurricane-costs.html).

638 National Oceanographic and Atmospheric Administration: Tropical Cyclone Rainfall, 2025.
639 <https://www.wpc.ncep.noaa.gov/tropical/rain/tcrainfall.html>.

640 Oasis Loss Modelling Framework: Oasis Loss Modelling Framework (Oasis LMF) [open-source catastrophe modelling
641 platform], 2025. <https://oasislmf.org>.

642 Oliver-Smith, A.: Hurricanes, Climate Change, and the Social Construction of Risk, *International Journal of Mass Emergencies
643 & Disasters*, 38, 1–12, 10.1177/028072702003800101, 2020.

644 Pesaresi, M. and Politis, P.: GHS-BUILT-S R2023A – GHS built-up surface grid, derived from Sentinel2 composite and
645 Landsat, multitemporal (1975–2030), 10.2905/9F06F36F-4B11-47EC-ABB0-4F8B7B1D72EA, 2023.
646 <https://data.jrc.ec.europa.eu/dataset/9f06f36f-4b11-47ec-abb0-4f8b7b1d72ea>.

647 Pilkington, S. F. and Mahmoud, H. N.: Using artificial neural networks to forecast economic impact of multi-hazard hurricane-
648 based events, *Sustainable and Resilient Infrastructure*, 1, 63–83, 10.1080/23789689.2016.1179529, 2016.

649 Qi, W., Yong, B., Ritchie, E. A., Tyo, J. S., and Toumi, R.: Global Increase of Tropical Cyclone Precipitation Rate Toward
650 Coasts, *Geophysical Research Letters*, 52, e2025GL115500, <https://doi.org/10.1029/2025GL115500>, 2025.

651 Rappaport, E. N.: Fatalities in the United States from Atlantic Tropical Cyclones: New Data and Interpretation, *Bulletin of the
652 American Meteorological Society*, 95, 341–346, <https://doi.org/10.1175/BAMS-D-12-00074.1>, 2014.

653 Schenkel, B. A., Chavas, D., Lin, N., Knutson, T., Vecchi, G., and Brammer, A.: North Atlantic Tropical Cyclone Outer Size
654 and Structure Remain Unchanged by the Late Twenty-First Century, *Journal of Climate*, 36, 359–382,
655 <https://doi.org/10.1175/JCLI-D-22-0066.1>, 2023.

656 Stansfield, A. M. and Reed, K. A.: Global tropical cyclone precipitation scaling with sea surface temperature, *npj Climate and
657 Atmospheric Science*, 6, 60, 10.1038/s41612-023-00391-6, 2023.

658 Stansfield, A. M., Reed, K. A., Zarzycki, C. M., Ullrich, P. A., and Chavas, D. R.: Assessing Tropical Cyclones’ Contribution
659 to Precipitation over the Eastern United States and Sensitivity to the Variable-Resolution Domain Extent, *Journal of
660 Hydrometeorology*, 21, 1425–1445, <https://doi.org/10.1175/JHM-D-19-0240.1>, 2020.

661 Tripathy, S. S., Jafarzaghan, K., Moftakhari, H., and Moradkhani, H.: Dynamic bivariate hazard forecasting of hurricanes for
662 improved disaster preparedness, *Communications Earth & Environment*, 5, 12, 10.1038/s43247-023-01198-2, 2024.

663 U.S. Bureau of Economic Analysis: Current-cost net stock of fixed assets and consumer durable goods [K1WTOTL1ES000],
664 2023. <https://fred.stlouisfed.org/series/K1WTOTL1ES000>.

665 U.S. Bureau of Economic Analysis: National Data Fixed Assets Accounts Tables, 2025.
666 https://apps.bea.gov/iTable/?reqid=10&step=3&isuri=1&table_list=16#eyJhcHBpZCI6MTAsInN0ZXBzIjpbMSwyLDMsM10sImRhdGEiOltbInRhYmxlX2xpc3QiLCIxNiJdLFsiQ2F0ZWdvcmlscyIsIIB1YmxpY0ZBQSJdLFsiU2NhbGUlLCItOSJdLFsiRmlyc3RfWVWVhciIsJjE5NTAiXSxbIkkxhc3RfWVWVhciIsJjIwMjMiXSxbIiNlcmllcyIsIkEiXV19.

669 U.S. Census Bureau: American Community Survey Housing Units by Year Built Variables — Tract, 2024.
670 https://hub.scag.ca.gov/datasets/41c90eef3a12451faff10c2a6b26fc46_2/about.

671 Vickery, P., J., Skerlj, P., F., Lin, J., Twisdale, L., A., Young, M., A., and Lavelle, F., M.: HAZUS-MH Hurricane Model
672 Methodology. II: Damage and Loss Estimation, *Natural Hazards Review*, 7, 94–103, 10.1061/(ASCE)1527-
673 6988(2006)7:2(94), 2006.

674 Wang, D., Chavas, D. R., and Schenkel, B. A.: Tropical cyclones expand faster at warmer relative sea surface temperature,
675 *Proceedings of the National Academy of Sciences*, 122, e2424385122, 10.1073/pnas.2424385122, 2025.

676 Wang, S. and Toumi, R.: On the relationship between hurricane cost and the integrated wind profile, *Environmental Research
677 Letters*, 11, 114005, 10.1088/1748-9326/11/11/114005, 2016.

678 Wang, S. and Toumi, R.: Recent migration of tropical cyclones toward coasts, *Science*, 371, 514, 10.1126/science.abb9038,
679 2021.

680 Wang, X., Verlaan, M., Apecechea, M. I., and Lin, H. X.: Computation-Efficient Parameter Estimation for a High-Resolution
681 Global Tide and Surge Model, *Journal of Geophysical Research: Oceans*, 126, e2020JC016917,
682 <https://doi.org/10.1029/2020JC016917>, 2021.

683 Ward, P. J., Blauhut, V., Bloemendaal, N., Daniell, J. E., de Ruiter, M. C., Duncan, M. J., Emberson, R., Jenkins, S. F.,
684 Kirschbaum, D., Kunz, M., Mohr, S., Muis, S., Riddell, G. A., Schäfer, A., Stanley, T., Veldkamp, T. I. E., and Winsemius,
685 H. C.: Natural hazard risk assessments at the global scale, *Nat. Hazards Earth Syst. Sci.*, 20, 1069–1096, 10.5194/nhess-20-
686 1069-2020, 2020.

687 Wehner, M. F. and Kossin, J. P.: The growing inadequacy of an open-ended Saffir–Simpson hurricane wind scale in a warming
688 world, *Proceedings of the National Academy of Sciences*, 121, e2308901121, 10.1073/pnas.2308901121, 2024.

- 689 Weinkle, J., Landsea, C., Collins, D., Musulin, R., Crompton, R. P., Klotzbach, P. J., and Pielke, R.: Normalized hurricane
690 damage in the continental United States 1900–2017, *Nature Sustainability*, 1, 808–813, 10.1038/s41893-018-0165-2, 2018.
- 691 Welker, C., Rössli, T., and Bresch, D. N.: Comparing an insurer's perspective on building damages with modelled damages
692 from pan-European winter windstorm event sets: a case study from Zurich, Switzerland, *Nat. Hazards Earth Syst. Sci.*, 21,
693 279–299, 10.5194/nhess-21-279-2021, 2021.
- 694 Wilson, K. M., Baldwin, J. W., and Young, R. M.: Estimating Tropical Cyclone Vulnerability: A Review of Different Open-
695 Source Approaches, in: *Hurricane Risk in a Changing Climate*, edited by: Collins, J. M., and Done, J. M., Springer International
696 Publishing, Cham, 255–281, 10.1007/978-3-031-08568-0_11, 2022.
- 697 Wong-Parodi, G. and Garfin, D. R.: Hurricane adaptation behaviors in Texas and Florida: exploring the roles of negative
698 personal experience and subjective attribution to climate change, *Environmental Research Letters*, 17, 034033, 10.1088/1748-
699 9326/ac4858, 2022.
- 700 World Meteorological Organization: WMO Atlas of Mortality and Economic Losses from Weather, Climate and Water
701 Extremes (1970–2019), <https://library.wmo.int/idurl/4/57564>, 2021.
- 702 WorldPop: Global High Resolution Population Denominators Project [dataset], 10.5258/SOTON/WP00674, 2018.
- 703 Zhong, Q., Gan, J., Tu, S., Toumi, R., and Chan, J. C. L.: Global increase in rain rate of tropical cyclones prior to landfall,
704 *Nature Communications*, 17, 114, 10.1038/s41467-025-68070-z, 2026.
- 705 Zuzak, C., Goodenough, E., Stanton, C., Mowrer, M., Ranalli, N., Kealey, D., and Rozelle, J.: National risk index technical
706 documentation, 2021. <https://hazards.fema.gov/nri/>.
- 707